

A novel Molecularly Imprinted Sensor based on Gold Nanoparticles/Reduced Graphene Oxide/Single-Walled Carbon Nanotubes Nanocomposite for the Detection of pefloxacin

Xiaohong Shi^{1,*}, Yu Zuo¹, Xiaoqing Jia¹, Xuemiao Wu¹, Ning Jing¹, Bin Wen¹, Xianwen Mi²

¹ Department of Chemistry, Taiyuan Normal University, Jinzhong 030619, China

² Faculty of Laboratory Medicine, Hunan University of Medicine, Huaihua, 418000, China

*E-mail: xiaohongshixhs@163.com

Received: 13 June 2020 / Accepted: 7 August 2020 / Published: 31 August 2020

A molecularly imprinted electrochemical sensor was developed for the detection of pefloxacin. The molecularly imprinted polymer (MIP) was prepared via electrodeposition on the surface of a gold nanoparticles/reduced graphene oxide/single-walled carbon nanotubes modified glass carbon electrode by incorporation of pefloxacin as a template molecule during the electrochemical polymerization of o-phenylenediamine. The nanocomposite of gold nanoparticles/reduced graphene oxide/single-walled carbon nanotubes was obtained by one-step electrochemical reduction. Differential pulse voltammogram (DPV) showed a linear pefloxacin concentration range from 5.0×10^{-7} mol/L to 2.0×10^{-5} mol/L, and the detection limit was 1.6×10^{-8} mol/L. The sensor also showed high selectivity, stability and reproducibility. Moreover, the sensor was successfully applied in the analysis of actual milk samples with satisfactory recovery rates.

Keywords: molecularly imprinted polymer (MIP); electrochemical sensor; pefloxacin; gold nanoparticles/ reduced oxide graphene/ single-walled carbon nanotubes

1. INTRODUCTION

Synthetic fluoroquinolones (FQs) are an important class of antibiotics used to treat multiple bacterial infectious diseases [1,2]. FQs kill bacteria by acting on two bacterial enzymes, DNA gyrase (topoisomerase II) and topoisomerase IV, which control the synthesis and replication of bacterial DNA [3,4]. Pefloxacin, [1-ethyl-6-fluoro-7-(4-methyl-piperazin-1-yl)-4-oxo-quinoline-3-carboxylic acid mesylate], is a second-generation of fluoroquinolone antibiotics and has a broad antibacterial spectrum and strong antibacterial activity [5,6]. Pefloxacin is used to treat respiratory, gastrointestinal and urinary infectious diseases in humans and is also used in veterinary medicine to treat microbial infections in livestock [7]. Unfortunately, as with other antibiotics, pefloxacin is misused or illegally used as a growth

promoter in poultry due to its antibacterial effects and low price [8]. The abuse of pefloxacin leads to high residues in animal products, wastewater, sewage sludge and soil,¹ which puts ecosystems as well as animal and human health at risk due to the potential increase in bacterial resistance [5,9]. Resistant bacteria can multiply in the human body or transfer resistance genes to other bacteria by means of the food chain [10]. Antibacterial agents run the risk of efficacy losses due to this increased resistance. Therefore, it is extremely important to develop a sensitive, low-cost and easy method for the rapid detection of pefloxacin in different environments (wastewater, animal derived food, sediment, etc.).

Currently, several analytical methods have been proposed for pefloxacin detection, such as high-performance liquid chromatography [11], ultrahigh performance liquid chromatography-tandem mass spectrometry [12], fluorescence [13], chemiluminescence [14], longitudinal surface plasmon resonance [15], capillary electrophoresis electrochemiluminescence [16] and electrochemical assay [17]. Among these approaches, electrochemical assay is an attractive method that has been widely used in many fields due to its simple operation, low cost, short analysis time and high sensitivity [18, 19]. Several reports involving electroanalytical techniques used for the determination of other fluoroquinolones such as ciprofloxacin, enrofloxacin, danofloxacin, levofloxacin, and ofloxacin, have been published [20, 21]. However, only adsorptive stripping voltammetry has been reported for the detection of pefloxacin [17]. Although the sensitivity of the abovementioned work for pefloxacin detection is high, routine use of the technique may be limited due to the use of a toxic mercury working electrode as well as the need for improvement in selectivity. Therefore, the development of an electrochemical method that is less toxic or nontoxic and highly selective is crucial for pefloxacin detection.

Molecularly imprinted polymers (MIPs) are a type of synthetic material prepared by copolymerization of a functional monomer, a cross-linker and a template molecule [22]. During MIP synthesis, a crosslinked polymer network is formed by covalent and/or noncovalent interactions between the functional monomer and the template molecule. After subsequent removal of the template molecules, binding cavities that are complementary in size, shape and functional groups to the template molecules are created within the network. The template can be the analyte itself, which generates molecular memory in the polymer and allows them to rebind the analyte with very high specificity [23, 24]. MIPs have been used widely in a variety of fields; the first report on molecularly imprinted sensing was published in 1993, and MIPs have experienced wide and rapid exploration for sensor fabrication since then [23, 25]. Compared with other recognition systems, molecularly imprinted polymers possess three major advantages: structure predictability, recognition specificity and application universality [24]. In particular, electrochemical synthesis of MIPs directly on the electrode surface has advantages, such as simple and rapid preparation as well as tunable control of the film thickness [26, 27]. Commonly used electroactive monomers for MIPs include, but are not limited to pyrrole, o-phenylenediamine, 4-aminophenol and boronic acid [22].

To improve the sensitivity of molecularly imprinted electrodes, nanomaterials such as graphene, carbon nanotubes and noble metal nanoparticles have been introduced to the MIP films [28]. Graphene, a two-dimensional material with a honeycomb-like network structure, is attractive for the development of electrochemical sensors by virtue of its unusual electrochemical properties, large surface area and good biocompatibility [29]. Gold nanoparticles (AuNPs) have been widely used to modify electrodes for amplifying signals in electrochemical sensors due to their excellent conductivity, easy synthesis and

tunable dimensions [30]. Unfortunately, AuNPs usually tend to aggregate owing to their high surface energy, so it is necessary to achieve a homogeneous distribution by introducing proper materials. Single-walled carbon nanotubes (SWCNTs) are composed of a single graphite sheet wrapped into a tubular structure with nanometer diameters; they also possess unique electronic properties, large specific surface areas, suitable mechanical properties and high chemical stability. These specific properties make SWCNT material very attractive for a variety of fields, particularly for use as electrode material [31]. Nanocomposites of graphene-SWCNTs not only prevent the formed reduced graphene oxide (RGO) sheets from aggregation and restacking, but can also be used as a scaffold to disperse AuNPs homogeneously [32].

The aim of this study was the development of a novel molecular imprinting electrochemical sensor for the sensitive and selective detection of pefloxacin. Gold nanoparticles, reduced graphene oxide and single-walled carbon nanotubes were introduced during the preparation of the imprinted sensor to provide a high specific surface area, high electrical conductivity and adhesion to the electrode to enhance its sensitivity. The sensing electrode was modified with gold nanoparticles/single-walled carbon nanotubes/reduced oxide graphene by one-step electroreduction and subsequent electropolymerization of o-phenylenediamine in the presence of pefloxacin. Importantly, the fabricated MIP sensor was used to detect pefloxacin in commercial milk to evaluate its feasibility for practical applications.

2. EXPERIMENTAL

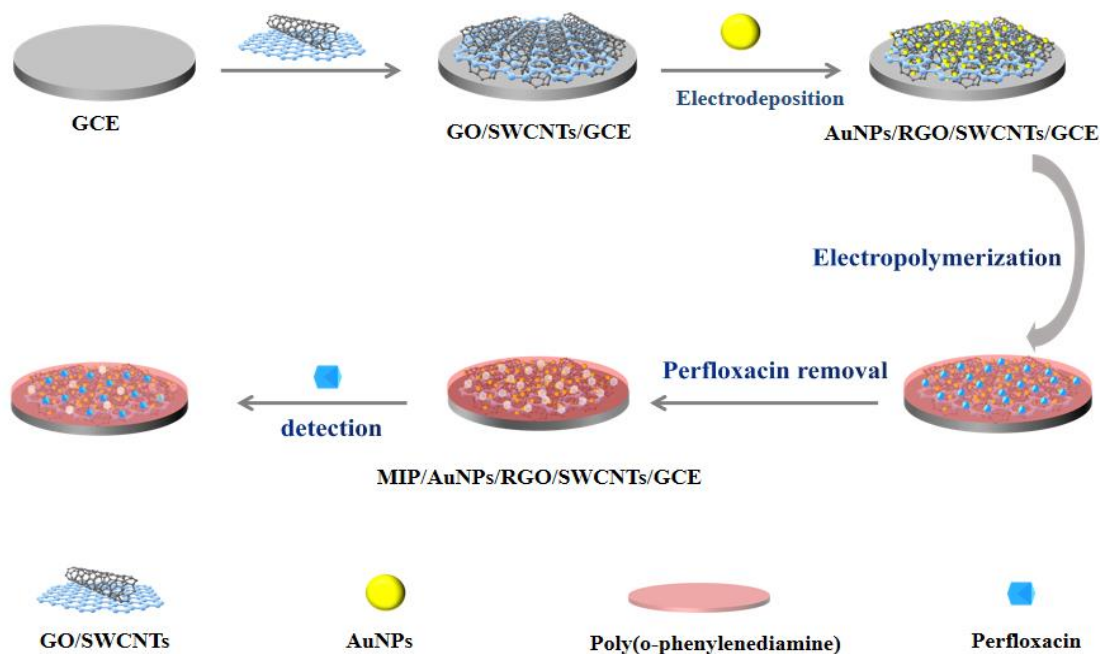
2.1 Reagents

Gold chloride trihydrate, o-phenylenediamine, pefloxacin mesylate dihydrate, enrofloxacin, ciprofloxacin hydrochloride, ampicillin, tetracycline hydrochloride and glucose were purchased from Aladdin Chemistry Co., Ltd. (Shanghai, China). Graphene oxide and carboxy-single walled carbon nanotubes were obtained from Nanjing Xfnano materials Co., Ltd. (Nanjing, China). Potassium ferricyanide ($K_3[Fe(CN)_6]$) and potassium ferrocyanide ($K_4[Fe(CN)_6]$) were purchased from Tianjin Hengxing Chemical Reagent Co. Ltd. (Tianjin, China). An acetic acid buffer solution (pH 5.0, 0.1 mol/L) was prepared by mixing the solutions of 0.1 mol/L acetic acid and 0.1 mol/L sodium acetate. All chemicals were of analytical grade. All solutions were prepared with double-distilled water.

2.2 Preparation of MIP modified electrodes

Prior to use, glassy carbon electrodes were polished carefully with 0.3 μm and 50 nm alumina powder to a mirror-like surface, and then washed successively with ultrapure water and ethanol. Scheme 1 outlines the fabrication procedure of the MIP-modified electrode. The clean glassy carbon electrode was coated using 5 μL of 0.5 mg/mL carboxylated SWCNTs and graphene oxide and then dried with an infrared lamp. Then, the gold nanoparticles/single-walled carbon nanotubes/reduced oxide graphene nanocomposite was electrodeposited onto the modified electrode surface by cyclic voltammetry (10 cycles) using a potential from -1.5 to 0.5 V, and a scan rate of 50 mV/s in 1 mmol/L HAuCl_4 . The MIP

film was prepared by electropolymerization of a 0.1 mol/L acetate buffer solution containing 5 mmol/L o-phenylenediamine and 10 mol/L pefloxacin using cyclic voltammetry (CV) from 0.2 V to 1.8 V at a scan rate of 50 mV/s for 15 cycles. The resulting pefloxacin-imprinted electrode was washed with ultrapure water and dried with nitrogen gas. Finally, the template molecules (pefloxacins) were extracted from the MIP film by submersion in a NaOH/ethanol (1:3, v/v) solution under slow stirring for 10 min followed by washing with double-distilled water. The pefloxacin-imprinted electrode was fabricated and used as the working electrode. A non-molecularly imprinted polymer (NIP) electrode was prepared under the same conditions without pefloxacin.



Scheme 1. Schematic illustration of the fabrication procedure for the MIP sensor and for pefloxacin detection. Definition: GCE, glass carbon electrode; GO, graphene oxide; SWCNTs, carboxylated-single walled carbon nanotubes; RGO, reduced graphene oxide; MIP, molecularly imprinted polymer.

2.3 Electrochemical measurements

Electrochemical measurements of cyclic voltammetry (CV) and differential pulse voltammetry (DPV) were performed using a CHI 660e electrochemical workstation (Chenhua, Shanghai, China) in a conventional three-electrode cell with a modified MIP-GCE as the working electrode, a saturated calomel electrode (SCE) as the reference electrode and platinum wire as the counter electrode. The MIP-GCE was initially enriched using a selected concentration of pefloxacin solution for 14 min. Cyclic voltammetry was conducted in a 0.1 mol/L KCl solution containing 2 mmol/L $K_3[Fe(CN)_6]/K_4[Fe(CN)_6]$ (1:1). The redox reaction of $K_3[Fe(CN)_6]/K_4[Fe(CN)_6]$ occurred on the working electrode surface. When pefloxacin was present in the detection solution, the MIP electrode could bind the pefloxacin. The pefloxacins prevented the redox reaction from occurring, and the peak current reduction was directly related to the pefloxacin concentration. DPV was used for quantitative detection of

pefloxacin because it provided a higher resolution of the electric signal, minimized double layer effects and enhanced sensitivity. In these analyses, the DPV potential range was 0.0–0.5 V, the amplitude was 0.05 V, the potential increment was 0.004 V, and the pulse width was 0.05 s.

2.4 Detection of pefloxacin in milk samples

Milk samples were purchased from a local supermarket. A 2 mL milk sample was added to 8 mL of an acetic acid buffer solution (pH 5.0) and vortexed for 1 min. The supernatant of the diluted milk samples was collected by centrifugation at 10,000 rpm and filtered through a 0.22 μm Millipore membrane. Next, 10 μL of varying pefloxacin concentrations were added to the milk samples and the amount of pefloxacin was detected according to the procedure described in the electrochemical measurement section in this article.

3. RESULTS AND DISCUSSION

3.1 Electropolymerization of the MIP electrodes

Cyclic voltammetry was used for electropolymerization of MIP and NIP films on the AuNPs/RGO/SWCNTs modified electrode in a 0.1 mol/L acetate buffer solution (pH 5.0). As shown in Figure 1, there was no obvious difference between the MIP and NIP electrodes. Irreversible oxidation was observed for both.

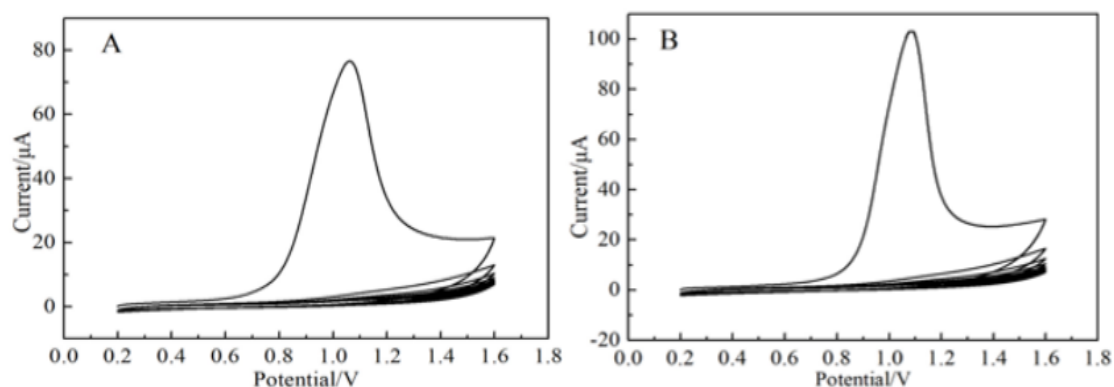


Figure 1. Cyclic voltammogram electropolymerization of (A) o-phenylenediamine in the presence of pefloxacin onto AuNPs/RGO/SWCNT/GCE in a 0.1 mol/L acetate buffer solution (pH = 5.0); (B) o-phenylenediamine onto AuNPs/RGO/SWCNT/GCE in a 0.1 mol/L acetate buffer solution (pH = 5.0)

The oxidation peak current decreased significantly as the number of scanning cycles increased, implying that a polymer film had formed on the working electrode. The pefloxacin molecules were trapped in the polymer film via the formation of hydrogen bonds and π - π interactions between pefloxacin and o-phenylenediamine. After electropolymerization, the MIP electrode with imprinted pefloxacin was

prepared by further elution. The size and shape of the imprinted cavity were determined during the imprinting procedure. The resulting special cavity selectively detected pefloxacin molecules.

3.2 CV characterizations of the different electrodes

The electrochemical behavior of electrodes modified with different materials was investigated by cyclic voltammetry in a 0.1 mol/L KCl solution containing 2 mM $[\text{Fe}(\text{CN})_6]^{3-/4-}$, a scan rate of 100 mV/s and a potential range of -0.4–0.8 V, and those results are shown in Figure 2. Two well-defined, reversible, $[\text{Fe}(\text{CN})_6]^{3-/4-}$ redox peaks were observed in the voltammograms of GO/SWCNTs/GCE (curve a). After electroreduction of the AuNPs-RGO-SWCNTs nanocomposite on the GCE surface, both peak currents in the anodic and cathodic curves increased slightly (curve b). This phenomenon was attributed to the larger electrochemically active surface area and the higher conductivity of the AuNPs-RGO-SWCNTs nanocomposite compared to GO-SWCNTs. However, the $[\text{Fe}(\text{CN})_6]^{3-/4-}$ redox peaks clearly decreased (curve c) when the electrode was covered with a polymer film. The poor electrical conductivity of the poly (o-phenylenediamine) and pefloxacin film prevented electron transfer of $[\text{Fe}(\text{CN})_6]^{3-/4-}$ to the electrode surface. As shown in Figure 2 (curve d), the high current peak appeared again after the polymeric membrane modified electrode was eluted with a 1 mol/L NaOH and ethanol solution (1:3, v/v) for 10 min, which confirmed the efficient removal of template molecules, promoting the diffusion of $[\text{Fe}(\text{CN})_6]^{3-/4-}$ and subsequent electron transfer at the surface of the MIP /AuNPs/RGO/SWCNTs/GCE. When the MIP electrode was incubated in pefloxacin for 14 min, a low current signal was observed (curve e). This signal illustrated that the MIP electrode could rebind template molecules, which can block electron transfer to the electrode surface. The peak current (curve e) was larger than that after polymerization (curve c), because a small number of vacancies remained, which led to adsorption but did not reach saturation.

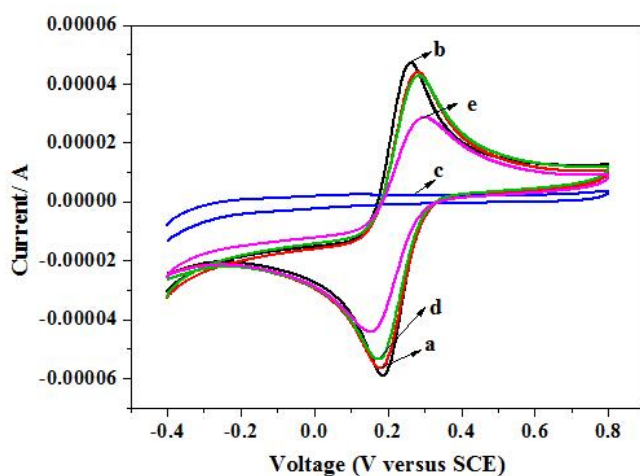


Figure 2. CV curves of different electrodes (a) GO/SWCNTs/GCE; (b) AuNPs/RGO/SWCNTs/GCE; (c) MIP/AuNPs/RGO/SWCNTs/GCE without the extraction of pefloxacin; (d) MIP/AuNPs/RGO/SWCNTs/GCE; (e) pefloxacin rebinding to the (d) after the detection process. The measurements were conducted in a 0.1 mol/L KCl solution containing 2 mM $[\text{Fe}(\text{CN})_6]^{3-/4-}$

3.3 Surface characterizations of the modified electrodes

The surface morphologies of the stepwise-modified electrodes were characterized by scanning electron microscopy (Hitachi SU8010, Japan) and are shown in Figure 3. Graphene oxide exhibits a typical flake-like structure, and long and tubular SWCNTs fill the graphene oxide sheets and form porous hybrid nanostructures (Figure 3A). This nanocomposite can prevent the subsequently formed reduced graphene oxide sheets from aggregating and restacking. Compared with the GO/SWCNTs modified electrode, Figure 3B shows that many granular AuNPs were uniformly distributed on the surface of the modified electrode following the electrochemical reduction. The electrode after electropolymerization (Figure 3C) was clearly covered with the rough polymeric membrane and is different from that before polymerization (Figure 3B). After removing the template molecules, the surface roughness of the MIP electrode notably increased (Figure 3D), indicating successful fabrication of the pefloxacin-imprinted electrode.

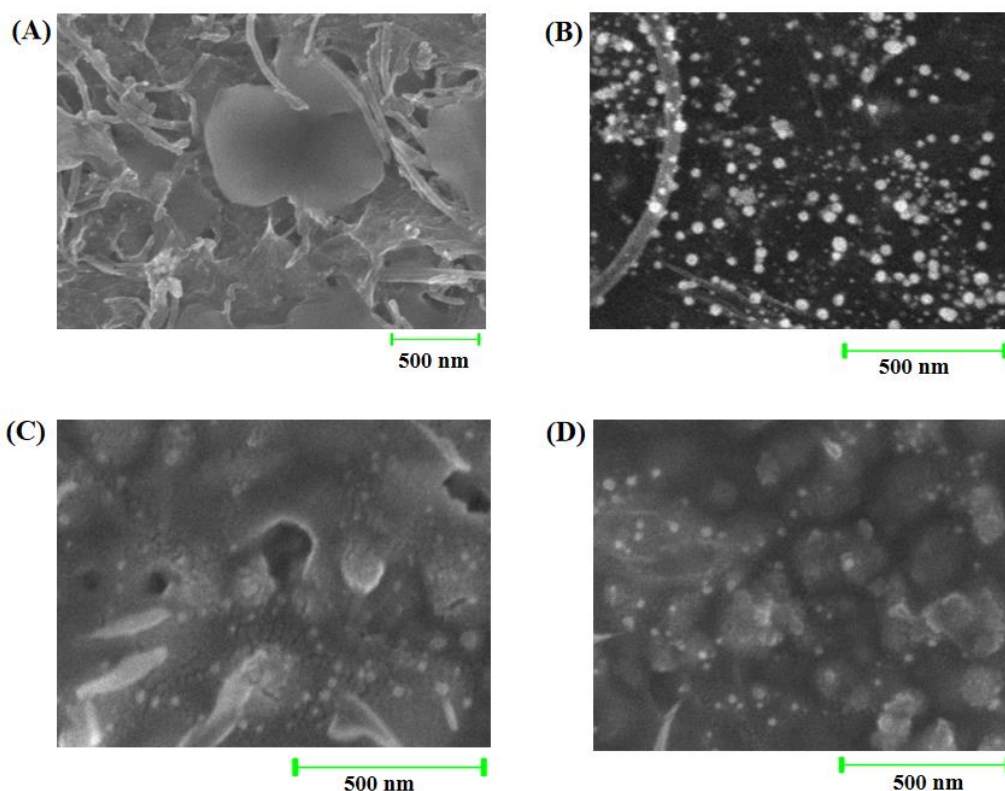


Figure 3. SEM images of different modified electrodes: (A) GO/SWCNTs; (B) AuNPs/RGO/SWCNTs; (C) MIP/AuNPs/RGO/SWCNTs before pefloxacin removal; (D) MIP/AuNPs/RGO/SWCNTs

3.4 Experimental parameter optimization for MIP sensor preparation

3.4.1 Optimization of the electroreduction and electropolymerization cycles

An investigation was conducted to determine how the electrical signal for the sensing of $1.0 \times$

10^{-6} mol/L pefloxacin was affected by the number of electroreduction cycles. The results are shown in Figure S1(A). The change in the intensity of the current generated by the AuNPs/RGO/SWCNTs/GCE increased as the number of electroreduction cycles of the AuNPs was increased from 2 to 8. However, when the number of electroreduction cycles exceeded 8, ΔI gradually decreased. Therefore, it was concluded that 8 electroreduction cycles was the optimum number. The reason for this result might be due to the decrease in the specific surface area of the electrode resulting from the aggregation of AuNPs on the electrode surface.

The number of electropolymerization cycles is an important factor in the fabrication procedure of a polymer membrane. The polymeric membrane thickness increased with the increasing number of scan cycles, and this thickness can affect sensitivity. Electropolymerization cycles ranging from 5 to 15 were examined and the results are shown in Figure S1(B). The largest signal response was obtained for 10 cycles. For 5 or 8 electropolymerization cycles, the imprinted polymer film was thin, fragile and the number of recognition sites was insufficient. However, too many cycles can also lead to a decrease in the response signal and resulted a membrane that is too thick. The pefloxacin molecules were not completely removed from the polymer matrix, which led to a decrease in the number of recognition sites. Therefore, the optimum polymerization cycle was found to be 10.

3.4.2 Effect of pH

To investigate the effect of the buffer solution pH on the response of pefloxacin detection, the sensor was tested in acetic acid buffer solutions with pH values varying from 3.0 – 7.0. As shown in Figure S2, the ΔI of the sensor for pefloxacin increased as the pH increased from 3.0 to pH 5.0, but decreased as the pH increased from pH 5.0 to 7.0. This behavior may be attributed to the weak interactions between monomers and templates at inappropriate pH values. Therefore, pH 5.0 was chosen as the optimum pH value for subsequent experiments.

3.4.3 Optimization of the incubation and elution times

The incubation time of the MIP sensor in the target molecule solution can affect the rebinding of the template molecule. The MIP sensor was incubated in a 0.1 mol/L acetic acid buffer solution containing 1 mmol/L pefloxacin; the response signal was recorded by the DPV. Peak currents were measured after 2, 6, 10, 14, 16 and 18 min incubation times. As shown in Figure S3(A), the response current decreased as the incubation time increased from 2 to 14 min. Incubation times longer than 14 min reduced and slowed the signal intensity change; this result indicated that the adsorption of pefloxacin by this MIP sensor reached saturation after 14 min. Hence, 14 min was selected as the optimal incubation time. It is very important to elute the template completely to obtain satisfactory sensitivity and selectivity. To optimize the template removal time, the electrodes were immersed in 20 mL of a 1 mol/L NaOH and ethanol solution (1:3, v/v) after electropolymerization for 2, 6, 10, 14 and 18 min. Figure S3(B) shows that response current increased with increasing elution time and remained virtually unchanged after 10 min, so this time was chosen as the suitable elution time for template removal.

3.5 Analytical performances of the developed sensor

3.5.1 Detection limit and linear range

Based on these optimized conditions, different concentrations of pefloxacin were detected using the developed molecularly imprinted sensor, and the detection results are shown in Figure 4A. The peak current for pefloxacin decreased gradually as the pefloxacin concentration increased, suggesting that some of the cavities in the molecularly imprinted membrane were filled with pefloxacin template molecules and prevented the diffusion and electron transfer of the redox probe. The number of cavities bound to pefloxacin was expected to be proportional to the ΔI , which can be calculated using Equation 1:

$$\Delta I = i_0 - i \quad (1)$$

where i_0 and i are the differential pulse voltammetry peak currents recorded by the same MIP electrode detected in the absence and presence of pefloxacin, respectively. The plot of ΔI vs. pefloxacin concentration is shown in Figure 4B. The linear range for pefloxacin detection was found to be from 5.0×10^{-7} mol/L to 2.0×10^{-5} mol/L. The calibration curve between the reduction peak current (ΔI) and the pefloxacin concentration (C) can be described by the equation $\Delta I (\mu A) = 1.32 C (\mu M) + 30.63$, $R^2 = 0.998$. The relative standard deviations of three parallel experiments ranged from 1.2–3.6%, indicating acceptable method repeatability. A detection limit of 1.6×10^{-8} mol/L was calculated as the ratio of three times the standard deviation of the blank measurements divided by the sensitivity.

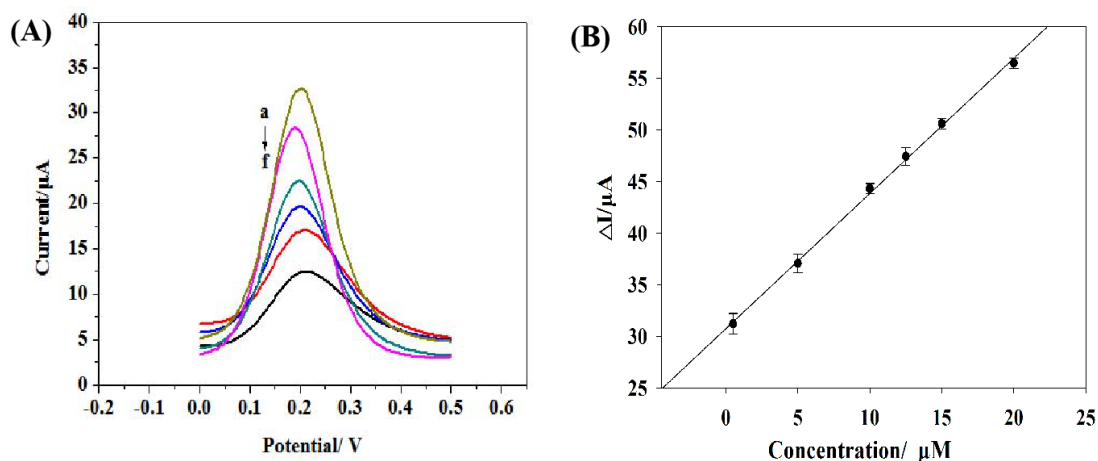


Figure 4. (A) Differential pulse voltammetry curves of the molecularly imprinted sensor after incubation with different concentrations of pefloxacin (a, 5.0×10^{-7} mol/L; b, 5.0×10^{-6} mol/L; c, 1.0×10^{-5} mol/L; d, 1.25×10^{-5} mol/L; e, 1.5×10^{-5} mol/L; f, 2×10^{-5} mol/L) in 0.1 mol/L acetic acid buffer solution (pH 5.0); (B) The calibration curve between the i_p and concentration of pefloxacin.

The comparison of the proposed sensor with other reported pefloxacin sensors is shown in Table 1. Compared with the time-resolved chemiluminescence method proposed by Murillo Pulgarín et al.[33], our sensor has the wider linear range and lower LOD for the detection of pefloxacin. The LOD of the immunochromatographic assay is lower than ours, but the required antibody is not specific for

pefloxacin [7]. As for Ahmed et al. proposed fluorescence assay [1], the parameters of the linear range and the LOD were inferior to our results. But the same two parameters of the fluorescence sensor developed by Du et al. were better than our results [35]. The detailed performance parameters of reported near-infrared spectroscopy [36] were not studied. The sensitivity of the spectrophotometry based methods [37,38] for the detection of pefloxacin was low, which could not meet the determination of many actual samples. The LOD of the three methods of surface-enhanced raman [39], longitudinal surface plasmon resonance [13] and capillary electrophoresis [40] was not detected. The LODs of the adsorptive stripping voltammetry proposed by Beltagi [17] and the differential pulse stripping voltammetry developed by Zhu et al. [41] were lower than our result, but the selectivity of the methods for the detection of pefloxacin was not as good as our sensor. This section is discussed in detail in the next section. The limits of detection of the differential pulse voltammetry and square wave voltammetry methods constructed by the Uslu [42] were 4.12×10^{-7} mol/L and 1.54×10^{-7} , respectively, which were not as good as our 1.6×10^{-8} mol/L. In summary, our proposed molecularly imprinted sensor showed a high sensitivity for the detection of pefloxacin compared with most other sensing methods.

Table 1. Comparison of the proposed sensor with other representative sensing methods

Sensing method	Linear/detection range	Limit of detection (LOD)	Selectivity for pefloxacin	Reference
Time-resolved chemiluminescence	25–250 $\mu\text{g/L}$ (5.37×10^{-8} – 5.37×10^{-7} mol/L)	13.7 $\mu\text{g/L}$ (2.94×10^{-8} mol/L)	No mention	[33]
Chemiluminescence enzyme immunoassay	No mention	0.23 $\mu\text{g/kg}$	No	[34]
Immuno chromatographic assay	2.5–50 ng/mL (5.37×10^{-9} – 1.07×10^{-7} mol/L)	0.082 ng/mL (1.76×10^{-9} mol/L)	No	[7]
Fluorescence	1.0×10^{-6} – 1.1×10^{-5} mol/L	2.4×10^{-7} mol/L	Yes	[1]
Fluorescence	4.0–900 ng/mL (8.61×10^{-9} – 1.93×10^{-6} mol/L)	0.8 ng/mL (1.7×10^{-9} mol/L)	No	[35]
Near-infrared spectroscopy	No mention	No mention	No	[36]
Spectrophotometry	2–18 $\mu\text{g/mL}$ (4.30×10^{-6} – 3.87×10^{-5} mol/L)	No mention	No	[37]
Spectrophotometry	10–45 $\mu\text{g/mL}$ (2.2×10^{-5} – 9.7×10^{-5} mol/L)	5.6 $\mu\text{g/mL}$ (1.2×10^{-5} mol/L)	No detection of relevant antibiotics	[38]
Surface-enhanced Raman	No mention	No mention	No	[39]
Longitudinal surface plasmon resonance	1–20 ng/mL (2.2×10^{-9} – 4.3×10^{-8} mol/L)	No mention	Yes	[13]

Capillary electrophoresis	No mention	No mention	No	[40]
Adsorptive stripping voltammetry	$1.0 \times 10^{-7} - 1.0 \times 10^{-9}$ mol/L	1.65×10^{-10} mol/L	No	[17]
Differential pulse stripping voltammetry	$4.0 \times 10^{-8} - 2 \times 10^{-7}$ mol/L	2.5×10^{-9} mol/L	No detection of relevant antibiotics	[41]
(1) Differential pulse voltammetry (2) Square wave voltammetry	$2.0 \times 10^{-6} - 2.0 \times 10^{-4}$ mol/L	(1) 4.12×10^{-7} mol/L (2) 1.54×10^{-7} mol/L	No	[42]
Differential pulse voltammogram	$5.0 \times 10^{-7} - 2.0 \times 10^{-9}$ mol/L	1.6×10^{-8} mol/L	Yes	This work

3.5.2 Selectivity, stability and reusability

To evaluate the selectivity of the proposed assay for detecting pefloxacin, interfering substances such as enrofloxacin, ciprofloxacin, tetracycline, ampicillin and glucose, were detected using our method. The concentration of all the detected antibiotics and glucose was 1.0×10^{-7} mol/L. There was no obvious signal change in the current before and after the addition of these interfering substances (Figure 5) except for pefloxacin, suggesting that the fabricated MIP sensor in this study possessed satisfactory selectivity, which was attributed to the matched cavities for pefloxacin molecules imprinted on the electrode surface of the sensor. From table 1, it can be seen that only the fluorescence assay proposed by Ahmed et al. [1], the longitudinal surface plasmon resonance developed by El-Kommos et al. and our sensor can highly selectively detect pefloxacin. But the LOD of our sensing method is the best among the three methods.

The sensor was stored at 4 °C when not in use. The response of the sensor to 1 µmol/L pefloxacin was reduced by only 6.64% compared with the initial response after one month, indicating the high stability of the sensor. The MIP/AuNPs/RGO/SWCNTs/GCE can be regenerated for pefloxacin detection by elution with a 1 mol/L NaOH and ethanol solution (1:3, v/v) for 10 min. The developed MIP sensor retained 96.5% of its initial response to pefloxacin after five runs.

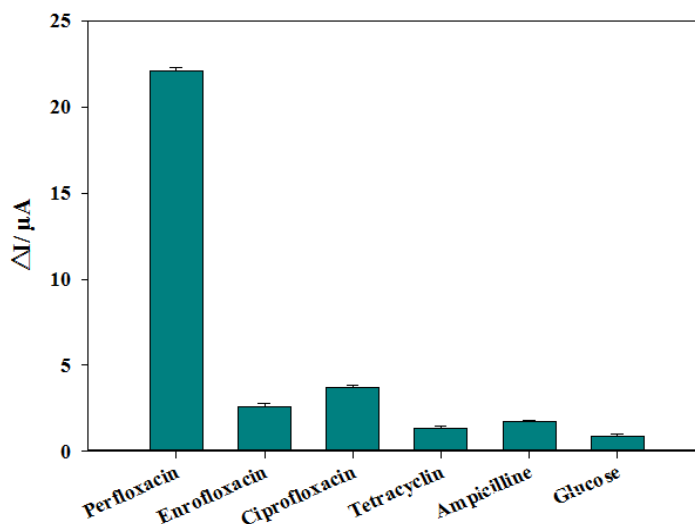


Figure 5. Changes in the current of the sensor in response to different interferences.

3.6 Analytical application

Table 2. Detection of pefloxacin in milk

Sample	Added (μM)	Found (μM)	Relative standard deviation %	Recovery %
1	1.00	0.87	3.25	87.0
2	5.00	4.55	0.70	91.1
3	10.00	9.62	0.77	92.0

To further evaluate the applicability of this method in practical sample analyses, different concentrations of pefloxacin were added separately to the milk samples, followed by detection using the developed sensor. The recovery rate of pefloxacin in the samples ranged from 87.0% to 92.0%, and the relative standard deviation ($n = 3$) was less than 5.0% (Table 2). This indicated that the fabricated MIP sensor could be successfully used for the detection of pefloxacin in milk.

4. CONCLUSIONS

In summary, a novel pefloxacin electrochemical MIP sensor was developed by electropolymerizing pefloxacin-imprinted poly(o-phenylenediamine) on a AuNPs/RGO/SWCNTs modified GCE. The fabrication of the MIP sensor was a simple and low-cost process. The proposed method provided a low detection limit and high pefloxacin specificity. Moreover, the sensor exhibited high stability, high reusability and acceptable application in actual milk samples. Therefore, this proposed method provides a new path for the specific detection of pefloxacin and potential applications in the food industry as well as in clinical and environmental fields.

SUPPORTING INFORMATION

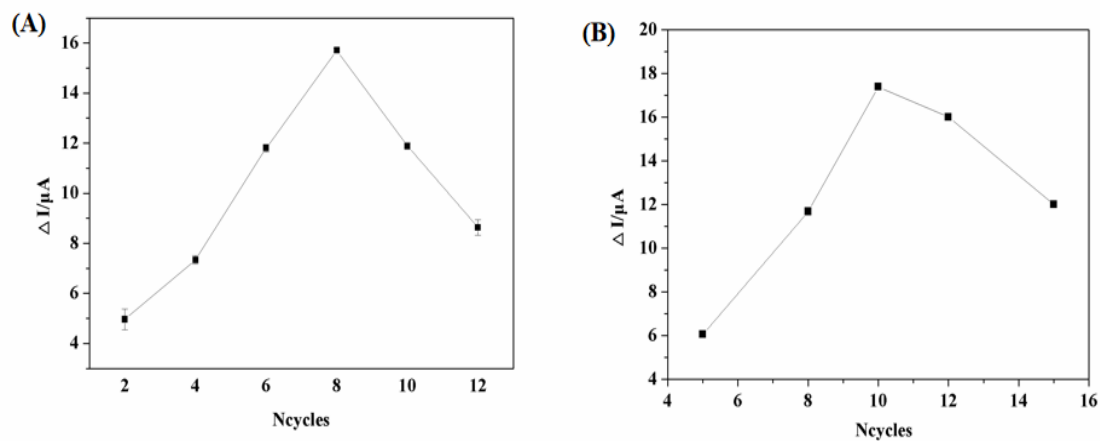
1. OPTIMIZATION OF THE ELECTROREDUCTION AND ELECTROPOLYMERIZATION CYCLES

Figure S1 Optimization of (A) the electroreduction cycles and (B) the electropolymerization cycles for the detection of 1.0×10^{-6} mol/L pefloxacin

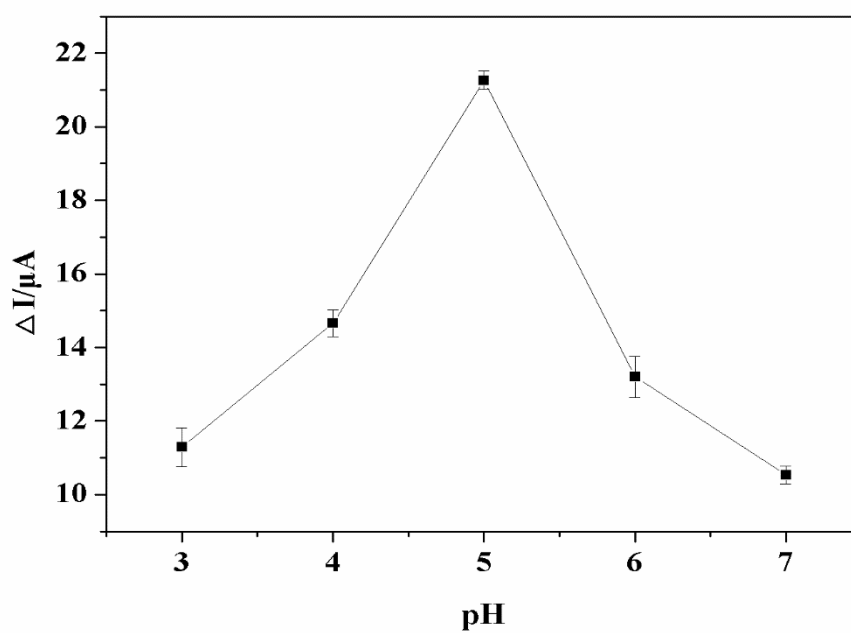
2. EFFECT OF PH

Figure S2. Effect of the pH on signal for the detection of 1.0×10^{-6} mol/L pefloxacin

3. OPTIMIZATION OF THE INCUBATION AND ELUTION TIMES

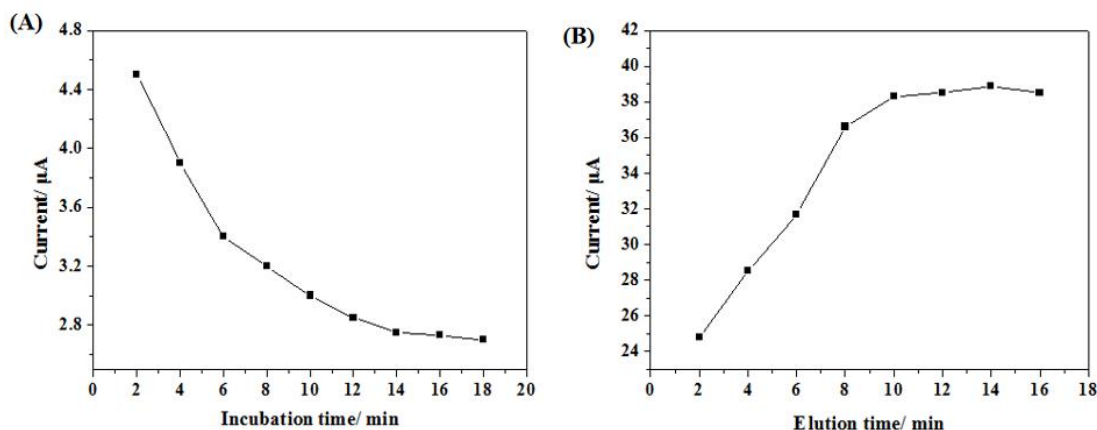


Figure S3. Effect of (A) incubation and (B) elution times on response signal

ACKNOWLEDGEMENTS

Financial support from the Scientific and Technological Innovation Programs of Higher Education Institutions in Shanxi (2019L0801, 2019L0818) and Natural Science Foundation of Hunan Province (2016JJ4062) are gratefully acknowledged.

References

1. F. Ahmed, A. Minhaz, M. Shah, N. Ain, A. Khan, K. Shah, S. Ullah, and M. Ishaq, *Microchem. J.*, 146 (2019) 332.
2. H. Yan, F. Qiao, and K. Row, *Anal. Chem.*, 79 (2007) 8242.
3. A. Gutierrez, S. Jain, P. Bhargava, M. Hamblin, M. Lobritz, and J. Collins, *Mol. Cell.*, 68 (2017) 1147.
4. L. Sun, L. Mei, H. Yang, K. Zhao, J. Li, D. Jiang, M. Li, and A. Deng, *Food. Anal. Method*, 9 (2016) 342.
5. Y. Zhou, Y. He, Y. Xiang, S. Meng, X. Liu, J. F. Yu, J. Yang, J. Zhang, P. Qin, and L. Luo, *Sci. Total. Environ.*, 646 (2019) 29.
6. G. Zhang, S. Zhang, B. Pan, X. Liu, and L. Feng, *Eur. J. Med. Chem.*, 143 (2018) 710.
7. D. Mukunzi, S. Suryoprabowo, S. Song, L. Liu, and H. Kuang, *Food. Agr. Immunol.*, 29 (2018) 484.
8. L. Sha, X. Tang, D. Liu, Y. Xu, Y. Ding, and F. Ding, *J. Food Protect.*, 81 (2018) 810.
9. F. Wang, Y. Feng, P. Chen, Y. Wang, Y. Sysisu, Q. Zhang, Y. Zeng, Z. Xie, H. Liu, Y. Liu, W. Lv, and G. Liu, *Appl. Catal. B-Environ.*, 227 (2018) 114.
10. A. Fàbrega, J. Sánchez-Céspedes, S. Soto, and J. Vila, *Int. J. Antimicrob. Ag.*, 31 (2008) 307.
11. Y. Zheng, Z. Wang, G. Lui, D. Hirt, J. Treluyer, S. Benaboud, R. Aboura, and I. Gana, *Biomed. Chromatogr.*, 33 (2019) e4506.
12. S. Susakate, S. Poapolathep, C. Chokeyaroenrat, P. Tanhan, J. Hajslova, M. Giorgi, K. Saimek, Z. Zhang, and A. Poapolathep, *J. Food. Drug. Anal.*, 27 (2019) 118.
13. M. El-Kommos, G. Saleh, S. El-Gizawi, and M. Abou-Elwafa, *Talanta*, 60 (2003) 1033.
14. P. Murillo, M. Alañón, and G. Jiménez, *Spectrochim. Acta. A*, 193(2018) 117.
15. X. Sun, L. Wu, J. Ji, D. Jiang, Y. Zhang, Z. Li, G. Zhang, and H. Zhang, *Biosens. Bioelectron.*, 47 (2013) 318.

16. B.Deng, L. Li, A.Shi, and Y. Kang, *J. Chromatogr. B.*, 877 (2009) 2585.
17. A. Beltagi, *J. Pharmaceut. Biomed.*, 31 (2003) 1079.
18. Z. Tasić, M. Petrović Mihajlović, M. Radovanovic, A. Simonović, and M. Antonijević, *J. Mol. Struct.*, 1159 (2018) 46.
19. A. Ghorbani, M. R. Ganjali, R. Ojani, and J. Raoof. *Int. J. Electrochem. Sci.*, 15 (2020) 2913.
20. D. Pinacho, F.Pinacho, M. Pividori, and M. Marco, *Sensors*, 14 (2014) 15965.
21. K. Abnous, N. Danesh, M. Alibolandi, M. Ramezani, S. Ramezani, and A. Emrani, *Sens. Actuator B-Chem.*, 240 (2017) 100.
22. P. Sharma, A. Pietrzyk-Le, F. D'Souza, and W. Kutner, *Anal. Bioanal. Chem.*, 402 (2012) 3177.
23. K. Haup, and K. Mosbach, *Chem. Rev.*, 100 (2000) 2495.
24. L. Chen, X. Wang, W. Lu, X. Wu, and J. Li, *Chem. Soc. Rev.*, 45 (2016) 2137.
25. E. Hedborg, F. Winquist, I. Lundstrom, L. Lundstrom, and K. Mosbach, *Sens. Actuator. A.*, 37-38 (1993) 796.
26. W. Lian, S. Liu, L. Wang, and H. Liu, *Biosens. Bioelectron.*, 73(2015) 214.
27. J. Erdőssy, V. Horváth, A. Yarman, F. Scheller, and R. Gyurcsányi, *Trac-Trends Anal. Chem.*, 79 (2016) 179.
28. W. Yang, K. Ratinac, S. Ringer, P. Thordarson, and J. Gooding, *Angew. Chem.-Int. Edit.*, 49 (2010) 2114.
29. Z. Xia, Y. Zhang, Q. Z. Li, H. J. Du, G. F. Gui, and G.Y. Zhao, *Int. J. Electrochem. Sci.*, 15 (2020) 559.
30. T. Xiao, J. Huang. D. Wang. T. Meng, and X. Yang, *Talanta*, 206 (2020) 120210.
31. B. Adhikari. M. Govindhan, and A. Chen, *Sensors.*, 15 (2015) 22490.
32. Y. Luo, F. Kong, C. Li, J. Shi. W. Lv, and W. Wang, *Actuator B-Chem.*, 234 (2016) 625.
33. J. Murillo Pulgarín, A. Alañón Molina, and E. Jiménez García, *Spectrochim. Acta. A.*, 193 (2018) 117.
34. X. Tao, M. Chen, H. Jiang, J. Shen, Z. Wang, X. Wang, X. Wu, and K. Wen. *Anal. Bioanal. Chem.*, 405 (2013)7477.
35. L. Du, A. Lin, and Y. Yang, *Anal. Lett.*, 37 (2004) 2175.
36. Y. Xie, Y. Song, Y. Zhang, and B. Zhao, *Spectrochim. Acta. A.*, 75 (2010) 1535.
37. S. Mostafa, M. El-Sadek, and E. Alla, *J. Pharmaceut. Biomed.*, 28 (2002) 173.
38. K. Basavaiah, and H. Prameela, *Indian. J. Chem. Tech.*, 9 (2002) 428.
39. Q. Shi, J. Huang, Y. Sun, R. Deng, M. Teng, Q. Li, Y. Yang, X. Hu, Z. Zhang, and G. Zhang, *Microchim. Acta*, 185 (2018) 84.
40. C. Fierens, S. Hillaert, and W. Van den Bossche, *J. Pharmaceut. Biomed.*, 22 (2000) 763.
41. M. Zhu, R. Li, M. Lai, H. Ye, N. Long, J. Ye, and J. Wang, *J. Electroanal. Chem.*, 857 (2020) 113730.
42. B. Uslu, B. Topal, and S. Ozkan, *Talanta*, 74 (2008) 1191.